International Academic Institute for Science and Technology

International Academic Journal of Science and Engineering
Vol. 5, No.1, 2018, pp. 170-190.
ISSN 2454-3896

International Academic Journal of Science and Engineering

www.iaiest.com

Investigating the effect of dimensions and distance of micro piles on the bearing capacity in a foundation settlement in gravel soils

Mehdi Ahmadi [a], Ahad Bagherzadeh Khalkhali [b], Hayl Radan [c], Behzad Dalili [d]

[a] *Master's degree in Civil Engineering-Geotechnics, Azad University, Electronic Unit. (corresponding author).*
[b] *Faculty Member, Islamic Azad University, Science and Research Branch, Civil Engineering Department, Tehran, Iran.*
[c] *Master's degree in Civil Engineering-Geotechnics, Azad University, Electronic Unit.*
[d] *Master's degree in Civil Engineering-Geotechnics, Azad University, Electronic Unit.*

Abstract

The piles are members of steel, concrete, reinforced concrete and wood, which is used to build a deep pile, if the landing capacity is not suitable for use. In spite of high costs, there are many cases in which there are numerous cases of pile sticks used to protect the building against sewage and other factors. The load on the pile is tolerated in two ways by the pile, part of which is tolerated by the side-pile resistance and the other part by the reciprocating tip of the pile. This composite system is called a piled raft system, or a piled raft foundation. In this research, Plaxis finite element software has been used to investigate the capacity of microfractory bearing. The results of this modeling show that the maximum displacement is about 3 mm, which occurred at the final modeling stage. In the first stage, the modeling of the level of displacement is very small, due to the grain size of the soil and the dry assumption of the material. In the second stage, the spatial variations show a sudden increase, due to the presence of pile s and the weight of the pile holder. In the third stage, the soil is completely compressed so that the forces have no significant effect on the summation, and the rate of the second stage and the third settlement are not significantly different.

Keywords: Micro fractures, Bearing Capacity, settlement, Plaxis

Received:24January 2018/Accepted:30 April 2018/Published:1 June 2018

Introduction

The piles are members of steel, concrete, reinforced concrete and wood, which is used to build a deep pile, if the landing capacity is not suitable for use. In spite of high costs, there are many cases in which there are numerous cases of pile used to protect the building against sewage and other factors. This compound system is called a piled raft system, or a pile-base, in short. Pile-Raft system bases are economically feasible because, when raft alone does not provide the required design in terms of cargo and storage, using multiple pillars under the raft, the amount of load capacity is increased and the overall settlement and differential settlement greatly reduced. The piles are divided into two groups of displacement piles and Replacement piles. Swinging piles are placed on the ground by knocking or vibration, and replaced by piles in pre-excavated places, prefabricated or in place. A microfiber is a replaceable pile by drilling and injection of cement slurry, which is usually flat and has a micro diameter (usually less than 300mm).

The phases of the throat include drilling a borehole, dipping and inserting artillery (pods and reinforcements) and injection of cement slurry. Thin fibers can be subjected to axial or lateral loads. Alternatively, they can be replaced by ordinary piles or as part of a plumb-soil composite mass, depending on the design method. Microfiber has made the use of this technology more effective in pushing the pixels up. One of these advantages can be short run time, improvement of specifications and load capacity of the soil and prevention of non-homogeneous settlements, creating the least disadvantages in the structure and the soil environment, creating the lowest noise during the operation, the ability to execute the minuscule, the ability to carry horizontal loads, and vertically pointed out that he has been encouraged by engineers in large construction projects, especially in coastal sand soils. In this study, the bearing capacity of piles in sandy soils has been investigated. Several studies have been carried out in this regard, some of which have been mentioned.

Salehi Malekshahi and Islami (2013) showed that the discrete piles act as soil hardening and that the sum of the piled raft system with soldered piles is close to that of the raft system with the attached piles.

Ghamari and Ghorbani (2010) investigated the microchip behavior under lateral static load using numerical modeling and the results of the model showed good agreement with the actual test results.

The Rasaei and Akhlaqi (2011) showed that micro piles are micro tube piles of less than 300 mm in diameter, which are carried out by drilling light steel armor and slurry injection. In their study, the behavior of microwave piles under vertical static load was investigated using abacus finite element software under nonlinear analysis.

Esmaeili Falak and Ramezani Yardi (2012) showed that the seismicity of the microscale slivers for the Phyllis soils is a complicated problem.

Negahdar et al. (1392) showed that limitation of suitable lands for the construction of necessary structures has led to the emergence of abundant methods for rehabilitation, improvement and strengthening of natural land conditions.

Hafez et al., with their studies, showed that various parameters of the structure have a significant effect on the micro-slab bending. Zincoe et al. (1998) and Taylor et al. (1998) showed that the microstructure can be improved by utilizing micro-pads.

Hedayati et al. (2012) showed that the use of piles in structures has a very wide range of uses, such as bridge bridges, tall buildings constructed on lose ground, Pipelines and it pointed out that piles are used to transfer loads from loose soils to resistant layers in greater depths.

Received:24January 2018/Accepted:30 April 2018/Published:1 June 2018

In recent years various laboratory and numerical methods have been used to study the buckling behavior of a pile. Batthcharia and Bolton have studied the failure of the piles in the rocks and examined the discrepancy between the findings of other researchers on the failure of the piles with their actual condition and condition. For example, one of the failures was the collapse of the Schwaukee Bridge piles in the 1964 Nigata earthquake. Many researchers such as Hamada in 1992 and Ishi Hara in 1993 saw the collapse of the bridge as a side extension. The position of this bridge is shown in Fig. 1 after its failure in Fig. 1 and its failure profile.

Figure 1 - The breakdown of the Schwaukee Bridge in the Niigata earthquake (Bhattacharya, 2003)

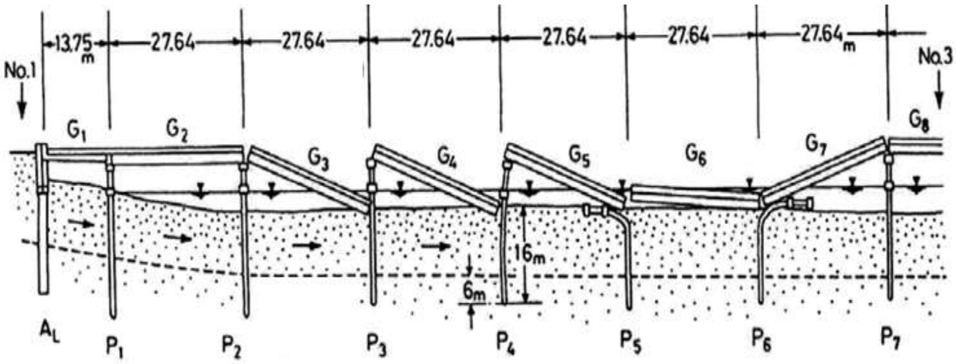

Figure 2 - A view of the deviations of the bridges of the Schwaukee bridge (Bhattacharya, 2003)

Hamid Reza Hashemi et al. (2011) have shown that several methods for analyzing Piled-Raft Systems have been presented, some of which are summarized by Poulos et al. (1997). Three classifications have been introduced for these methods: (1) simplified computational methods, (2) approximate computer methods, (3) more precise computer methods.

Received:24January 2018/Accepted:30 April 2018/Published:1 June 2018

Simplified computational methods are presented by Poulos and (1980) Davis, (1983, 1994) Randolph, Van Impe and Clerq (1995) and Burland (1995).

All of them include simplifying the modeling of soil profiles and loading conditions on the deck. Approximate computer methods include two methods: (1) the "strip on springs" method, in which the deck is routinely lined with strings that represent the hardness of the pile (e.g. 1991 Poulos) and (2)): The "plate on springs" method, in which the deck is designed as a plate and pile springs, such as Georgiadis and (1998, Anagnastopoulos; (1998, Viggiani; (1994 Poulos;) Randolph and (1993, Clancy.

Computer methods are more accurate based on numerical methods. These methods include four methods: (1) the boundary element method, where the piles and decks are both separate and use elastic theory (eg Wiesner and Brown 1975), (Banerjee and 1971 Butterfield), (Kuwabara 1989), (Sinha 1997); (2) Combined Boundary Elements for Pile and Finite Element for decks such as (Hain and 1987 Lee), (Ta and 1996 Small).

(3): Simplified finite element analysis, in which the foundation system is considered as a strain-strain problem (Desai 1974);

Van Impe (2001), analyzing a pile-deck foundation system, showed that there is a small correlation between the above-mentioned methods in the load-load diagram, especially in deformations. Of course, the graph obtained from the two-dimensional analysis of FLAC with other methods has a relatively large difference (Fig. 3).

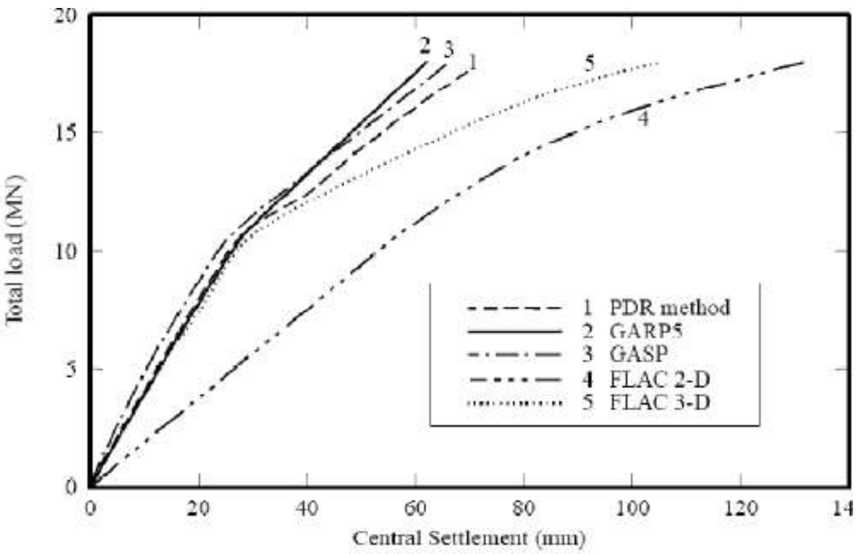

Figure 3 - Comparison of Different Analysis Methods of Piled raft Foundation Systems

2. Research method

2-1. Settlement and Allowed Resistance

Several theories are presented in relation to the final loading capacity of surface foundations. In the design of each foundation, the failure of the load capacity along with the settlement should be considered, but in designing most of the foundations there is a tolerance for the amount of authorized sewage. In the

Received:24January 2018/Accepted:30 April 2018/Published:1 June 2018

following diagram, the load diagram is based on the unit area of the foundation q in relation to the foundation S settlement. Given this figure, it can be seen that the final carrying capacity occurs at the S_u settlement. Now assume that S_{all} is the permitted sum of the foundation and q $_{(all\ (s))}$ of the corresponding carrying capacity. If F_s is the coefficient of reliability against the failure of the load capacity, then the load carrying capacity will be equal to q $_{(all\ (s))}$ = Fs / q (u) whereas the corresponding settlement with q $_{(all\ (b))}$ is equal to S'. For a foundation with a smaller width B, S' can be smaller than S_{all}, but for larger values of B, S '> S_{all}. Therefore, for micro -size foundations, the load capacity is controllable and in larger latitudes, the control session will be allowed.

Foundation settlement can have three components (note the last paragraph of the previous paragraph):

A) Elastic seat, Se, b) primary consolidation settlement, S_c, c) secondary consolidation settlement, S_s. So the total sum of St will be equal to:

$$S_t = S_e + S_c + S_s$$

In each foundation, some of these components can be zero or neglected.

Elastic sediments are due to dry soil deformation as well as moist and saturated soils without any change in moisture content. The initial consolidation settlement is a time dependent process that occurs in clay soils below the aquifer as a result of volumetric changes in soil due to the outflow of pore water. The secondary consolidation settlement occurs after the initial consolidation settlement in saturated clay soils, due to the shape of the plastic structure of the soil.

The three types of settlement discussed above are discussed in this chapter.

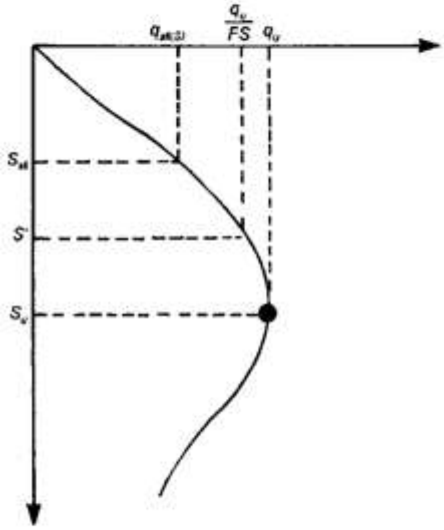

Figure 4 - Load curve - Surface foundation arrangement

2-2. an analysis of the size of the foundation and the load capacity of the foundation

2-2-1- Bearing capacity of soil below the pit

As stated above, the maximum tolerable stress in the subsoil soil is equal to q $_{(ult)}$ in this case the soil is placed on the verge of rupture. This value is directly related to the rupture of the subsoil. In fact, internal forces that are created on the surface of the rupture within the soil are the main factor of q $_{(ult)}$. To

Received:24January 2018/Accepted:30 April 2018/Published:1 June 2018

determine $q_{(ult)}$ from the surface of the rupture, we go through the steps below, which is called (partial equilibrium method).

1. We first guess the level of rupture in the subsoil soil.
2. We represent the forces on the level of rupture as a free object diagram.
3. Finally, by writing a proper equation of equation, we obtain $q_{(ult).}$

The general form of the relationship between determining the bearing capacity ($q_{(ult)}$) is:

q_{ult} = c N_c+ q N_q + 0.5 $B\gamma N_\gamma$

Which are respectively:

$$N_c = c[2k_p \cos(45 - \frac{\emptyset}{2}) + \sqrt{k_p}]$$

$$N_q = [k_p^{\frac{3}{2}} \cos(45 - \frac{\emptyset}{2})]$$

$$N_\gamma = [\frac{1}{2} k_p^2 \cos(45 - \frac{\emptyset}{2}) + \frac{\sqrt{kp}}{2}]$$

Most researchers argue that the precise coefficients N_c, N_q, N_γ are determined. These coefficients are a function of the internal friction angle of the soil. The above relation is the simplest form of the relation $q_{(ult)}$, which consists of three terms of adhesion, depth and width.

On the other hand:

$$N_c = (N_q - 1) \cot \emptyset$$

As it is studied in saturated soils, we study the relationships in saturated soils.

Hence, instead of the parameter γ, we use the parameter γ_e:

$$\gamma_e = \gamma' + \frac{d_w}{H}(\gamma - \gamma')$$

$$\gamma_w - \gamma_{sat} = \gamma'$$

In the above relation, γ 'is the soil immersion gravity γ is the unsaturated gravity of the soil.

d_w The distance between the water level below the foundation and the foundation.

H Effective Depth.

In saturated soils, the water level below the zero is equal to zero $\gamma_e = \gamma'$

2.2.2. Calculate the uniform pressure stresses foundation

In the case of the P load, which is then loaded right in the center of the substation, the distribution of stress below symmetry will be calculated in accordance with which compressive stress is calculated as follows.

$$q = \frac{P}{B * L}$$

Where B and L are respectively the width and length of the pseudo-length.

Now, if the load entered has a central exit, its calculation is done as follows.

$$q_{max} = \frac{P}{A} + \frac{M}{S} = \frac{P}{BL}(1 + \frac{6eB}{B})$$

$$q_{min} = = \frac{P}{A} - \frac{M}{S} = \frac{P}{BL}(1 - \frac{6eB}{B})$$

Received:24January 2018/Accepted:30 April 2018/Published:1 June 2018

Where the eB is the exit distance from the center of the load.
Now if there is a double axis bend under the influence of the following:

$$q = = \frac{P}{A} \pm \frac{M_x\, y}{I_x} \pm \frac{M_y\, x}{I_y}$$

In the above relation, x and y are the coordinates of the point below, and I_x and I_y, the moment of inertia is the cross section of the x and y axes.

2-3 Foundation settlement

Using the theory of elasticity, the elastic corners of a corner of a flexible rectangular foundation to dimensions

B * L or a circle of diameter B on the surface of the soil with infinite depth can be estimated using the following equation.

$$S_i = \frac{q \cdot B}{E_s}(1-\mu_s^2) \cdot I_1$$

Where in:

Reactionary settlement S

Poisson ratio of soil μ_s

Foundation width B

Q Contact Tension

Modulus of soil elasticity underlying foundation E_s

I_1 The coefficient of influence, which is a function of the L / B ratio, is calculated from the following equation.

$$I_1 = \frac{1}{\pi}\left[\frac{L}{B}\ln\left(\frac{1+\sqrt{(L/B)^2+1}}{L/B}\right) + \ln\left(\frac{L}{B}+\sqrt{(L/B)^2+1}\right)\right]$$

If we want to calculate the Flexible Center settlement using the above equation, we split the foundation into four equal parts, and after calculating the summit of the corner of one of the rectangles, we quadruple the resulting summation. In this way we have:

$L' = L / 2$ و $B' = B / 2$

As a result, the coefficient I_1 does not change, so the flexible FPC settlement can be calculated as follows:

$$S_{i(center)} = 4 \times \frac{qB'}{E_s}(1-\mu_s^2)I_1 = 4 \times \frac{qB}{2E_s}(1-\mu_s^2)I_1 \rightarrow I_{center} = 2I_1$$

Finally, the following relationships can also be used:

Received:24January 2018/Accepted:30 April 2018/Published:1 June 2018

$$S_{i(corner)} \approx 0.5S_{i(center)}$$
$$S_{i(average)} \approx 0.85S_{i(center)}$$
$$S_{i(rigid)} \approx 0.79S_{i(center)}$$
$$S_{i(rigid)} \approx 0.93S_{i(average)}$$

4. Plate bearing capacity

2.4.1 Bearing capacity of individual piles

The load on the pile is tolerated in two ways by the pile, part of which is tolerated by the side-pile resistance and the other part by the pile bearing retention resistance.

$$Q_{ult} = Qs + Q_P$$

Where Qs is the friction resistance of the body and $Q_{(p)}$ is the resistance of the pile.
Calculation of Fixed Resistance $Q_{(s)}$

$$Q_s = \int dQ_s = \int_{\cdot}^{l} f_s(z) P(z)\, d_z$$

In this regard $f_s(z)$ the maximum adjacent tensile strength on the aluminum faces and $P_{(z)}$ is the cross-sectional area of the element.

$$Q_s = P \int_{\cdot}^{l} f_s(z)\, d_z$$

In granular soils, the value of f_s is calculated as follows:

$$f_s = \mathrm{k}\, \sigma'_\vartheta \tan\delta$$

In the above equation, σ'_ϑ'is the effective soil stress in depth z and is a function of z.
The friction angle between the pile and the soil is always smaller than the internal friction angle (Ø) and is between 2/3 and 3/4 Ø.
Calculation of $\boldsymbol{Q_p}$ reciprocating end bearing

$$Q_p = A_p\, q_p = A_p\, (\mathrm{c}\, N_c + q'\, N_q)$$

In the above relation, A_ (p), Q_P, c and q' respectively, the pile section, soil bearing capacity at the tip of the pile, soil adhesion and effective vertical stress at the tip of the pile.
• The end resistance of the pile in granular soils

$$Q_p = A_p\, q'\, N_q$$

2.4: Calculate the efficiency and capacity of the bearing of the pile

$$Q_{ug} = E_g \sum Q_u$$

Received:24January 2018/Accepted:30 April 2018/Published:1 June 2018

In the above relation Q_{ug}, the bearing capacity of the pile and $\sum Q_u$, the total bearing capacity of each of the piles is normal, E_g is also the same (efficiency) of the pile group.

$$E_g = \frac{B_g * L_g \text{ Dimensions with single pile bearing capacity}}{\sum Q_u \text{ Single-Bearing pile Total Capacity}}$$

• Elastic settlement of the pile group

The easiest way to determine the elastic enclosure of the pile group is by (tight) as follows:

$$S_{g(e)} = \sqrt{\frac{B_g}{D}}\, S$$

In the equation mentioned: $S_{g(e)}$ Elastic settlement of the pile group B_g Pile band section width D*: The width or diameter of each single pile in the pile group*

S: A single pile of elastic settlement at the time of operation.

2-5: Modeling

To begin the modeling, we must validate the software as a whole, after validating and reaching the exact answers that are close to the results of past research, we are beginning to build new models. In order to validate the software used in this PIN, we will use the research done by Matsumoto et al.

Matsumoto et al. (2014) had a numerical analysis of the loading of pips in granular soils. In the model, the soil was rehabilitated with the aid of three 20-mm diameter piles.

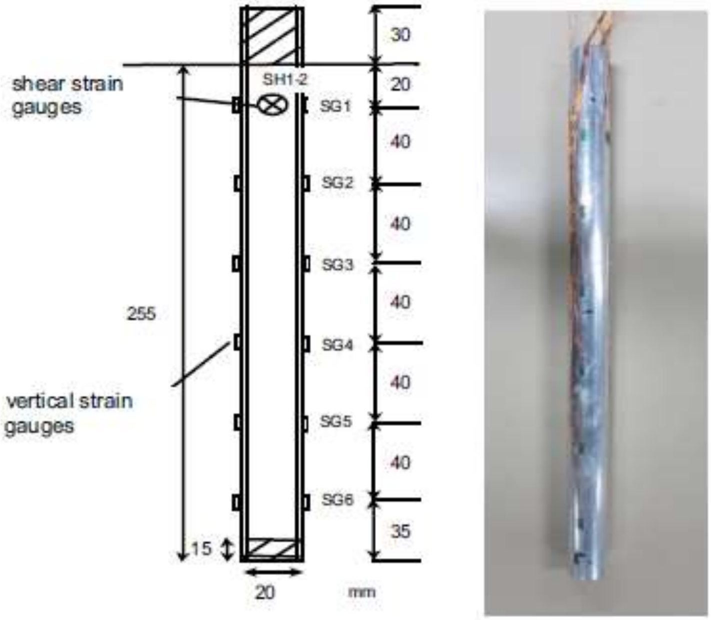

Figure 5 - piles used in Matsumoto et al

In this research, the loads borne by these three piles are tolerated. Their results showed that the operation of the pile significantly depends on the interaction between the piles, and the behavior of the piles cannot be considered separately.

Received:24January 2018/Accepted:30 April 2018/Published:1 June 2018

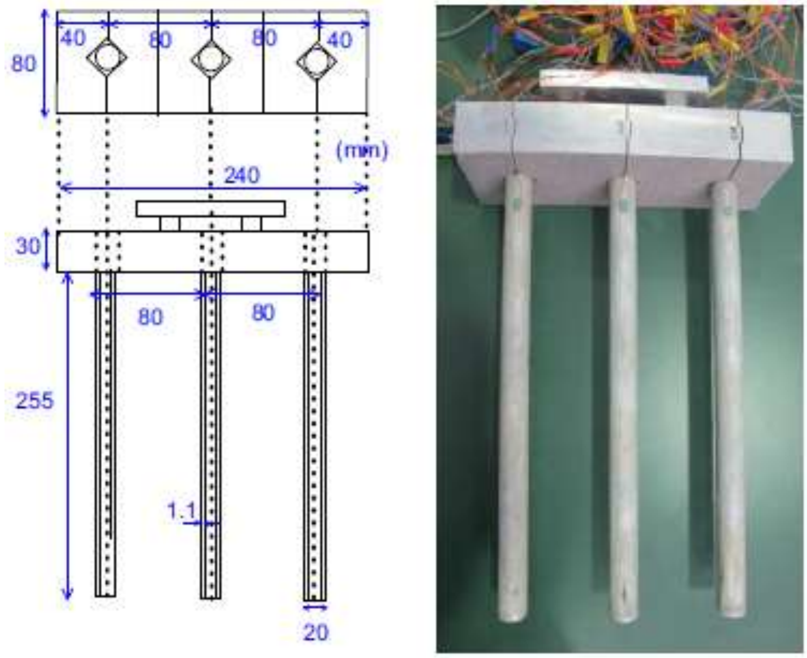

Figure 6 - How to put piles next to each other

In Plaxis software, in addition to their geometry, we also need mechanical specifications for modeling these piles. In the table below, in addition to the geometric characteristics of the piles, their mechanical properties are also specified.

Table 1. Geometric characteristics of the used piles

Item	Value
Outer diameter, D (mm)	20.00
Wall thickness, t (mm)	1.1
Length, L (mm)	255
Cross sectional area, A (mm^2)	65.31
2nd moment of inertia, I (mm^4)	2926.2
Young's modulus, E (N/mm^2)	64,000
Poisson's ratio, υ	0.31

They placed the desired pile in a soil sample at a height of 530 mm and a width of 800 and 500 mm in order to complete the laboratory set-up to complete the test.

Received:24January 2018/Accepted:30 April 2018/Published:1 June 2018

International Academic Journal of Science and Engineering,
Vol. 5, No. 1, pp. 170-190.

Table 2. Mechanical Properties of Soil examined by Matsumoto et al

Item	Value
Density of soil particles, ρ_s (t/m^3)	2.66
Maximum dry density, ρ_{dmax} (t/m^3)	1.542
Minimum dry density, ρ_{dmin} (t/m^3)	1.280
Maximum void ratio, e_{max}	1.079
Minimum void ratio, e_{min}	0.725
Median grain size, D_{50}	0.423
Coefficient of uniformity, U_c	1.880

By analyzing the vertical load on the piles, they analyzed their model and concluded that the use of pile-based piers will have a huge impact on performance improvement, including vertical transfer of piles and transferring these, it was repeatedly in the lower layers. The load bearing in different parts of the pile depends on the amount of tension that comes in.

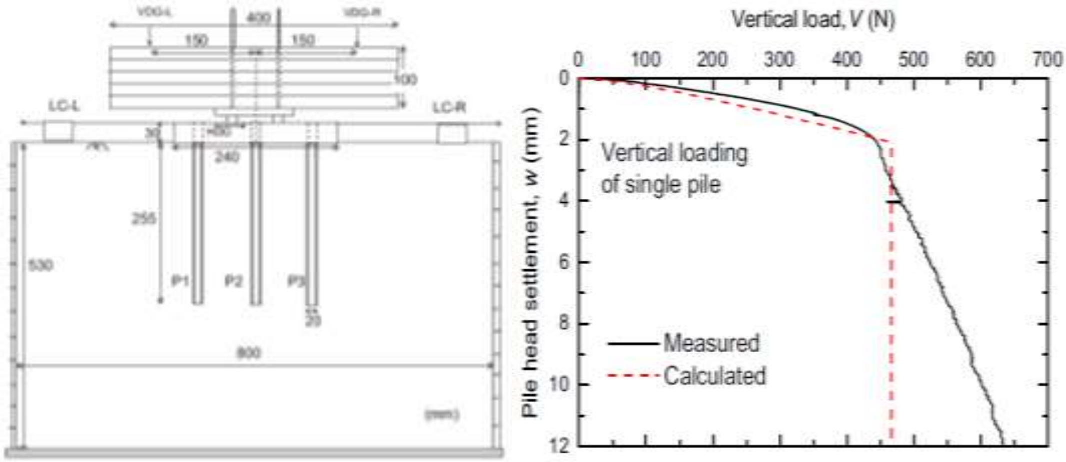

Figure 7 - Test setup and load diagrams obtained in Matsumoto et al

3. Results

To apply the boundary conditions, the displacement in horizontal direction is closed on the three sides of the model (Fig. 8) and the vertical displacement of the foundation is limited. The relationship between the pile and the foundation and the pile cap and the foundation line with the dot line are shown in Fig. In modeling with the Plaixs software, the displacement is generally closed in all three directions of the coordinate axis at the model floor, which means that the floor of the foundation is firmly ground to the ground. In the vertical walls of the foundation, the displacement is closed in the direction of the axis x and z, and only the possibility of changing in vertical direction exists.

Received:24January 2018/Accepted:30 April 2018/Published:1 June 2018

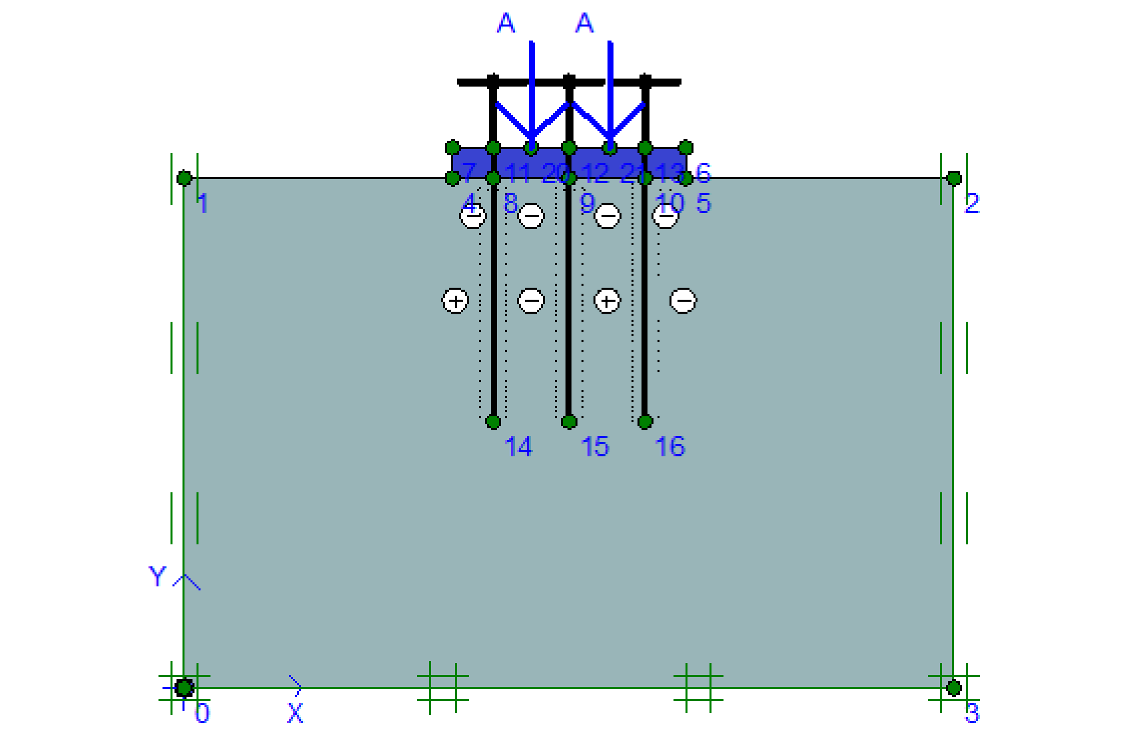

Figure 8 - Applying boundary conditions

Deformation rate

Further variations are presented in different stages. In each of three steps, the variations will occur according to the conditions described below.

First stage

The deformed foundation in the first phase is presented in Fig. 9. As shown in the figure, the deformation rate is very small in a 5-day interval without the use of piles, with a maximum displacement of 69e-12m. The variation in location is very small. The reason for this is that the size of the model is micro (the model was made on a laboratory scale), and secondly, the soil is considered as sand, which is not consolidated and the passage of time has no effect on the variation of the site, and on the other hand, dry has been assumed, and there is no blue for exiting, resulting in reduced volume. Another issue to be considered is lack of water, which increases the friction and slowness of the movement of sand particles on one another, resulting in a decrease in sowing. In saturated mode, the sand will experience greater spatial variation over time (this is true in all three stages).

Received:24January 2018/Accepted:30 April 2018/Published:1 June 2018

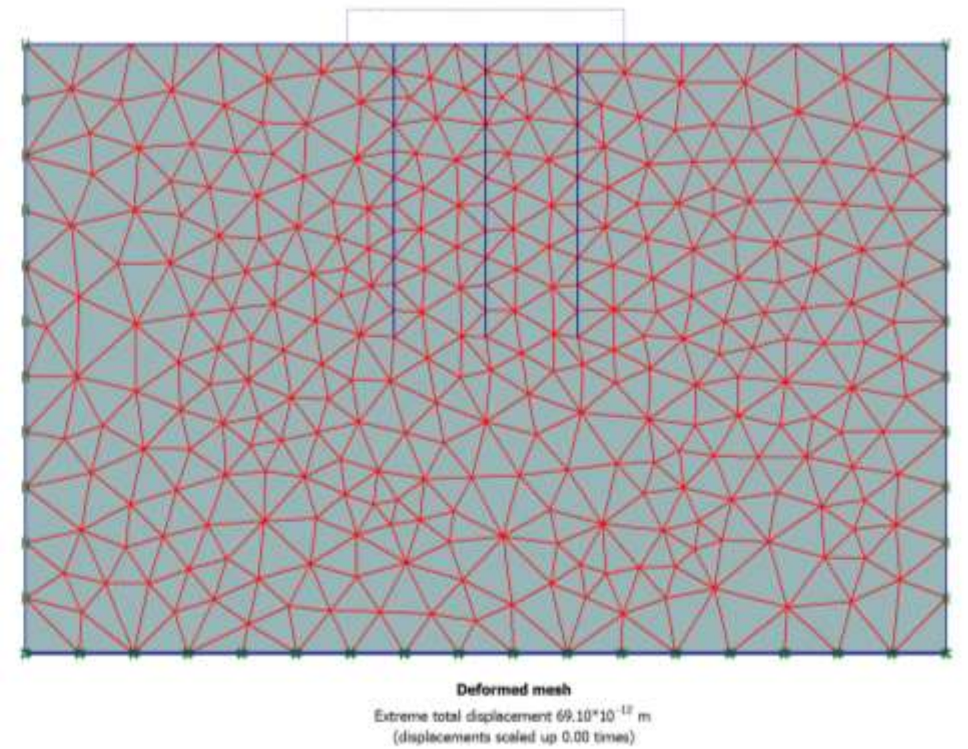

Figure 9 - Movable structures in the first stage

The deformation found by considering the presence of pile pins is presented in Fig. 10. The maximum displacement in the 5-day time interval was 2.7 mm, which is significant. The reason for this is the pressure caused by the presence of piles and their warts, which causes the soil to accumulate under this section. A very small part of this settlement is about consolidation and soil weight. At this point, the interaction between soil and piles has also been applied. The interaction between the warhead and the foundation will not affect the results because the earthquake load has not been applied (no movement and frictional force will be created), but the interaction between the piles and the foundation due to the friction created during the summit has a significant impact. For this reason, the results of this modeling are very carefully considered due to the involved interactions.

Received:24January 2018/Accepted:30 April 2018/Published:1 June 2018

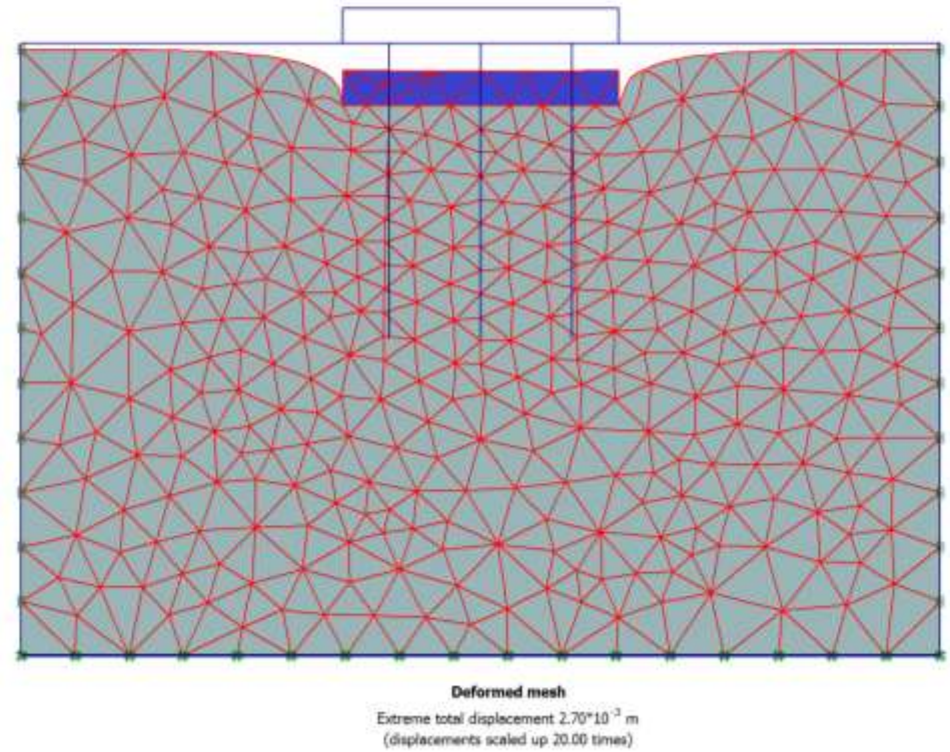

Figure **10 -** Modified structure in the second stage

Second stage

The deformation found in conjunction with the presence of piles, pile shells, and two point spots in the middle of the pile pins is presented in Fig. 11. The amount of loads is considered to be 700 N / m. The maximum displacement in the 9.5-day interval was 2.86 mm, which is significant. The change in location was not significantly different from the previous one. The reason for this is that the soil has been completely compressed during the previous steps and its application has not reduced significantly.

Received:24January 2018/Accepted:30 April 2018/Published:1 June 2018

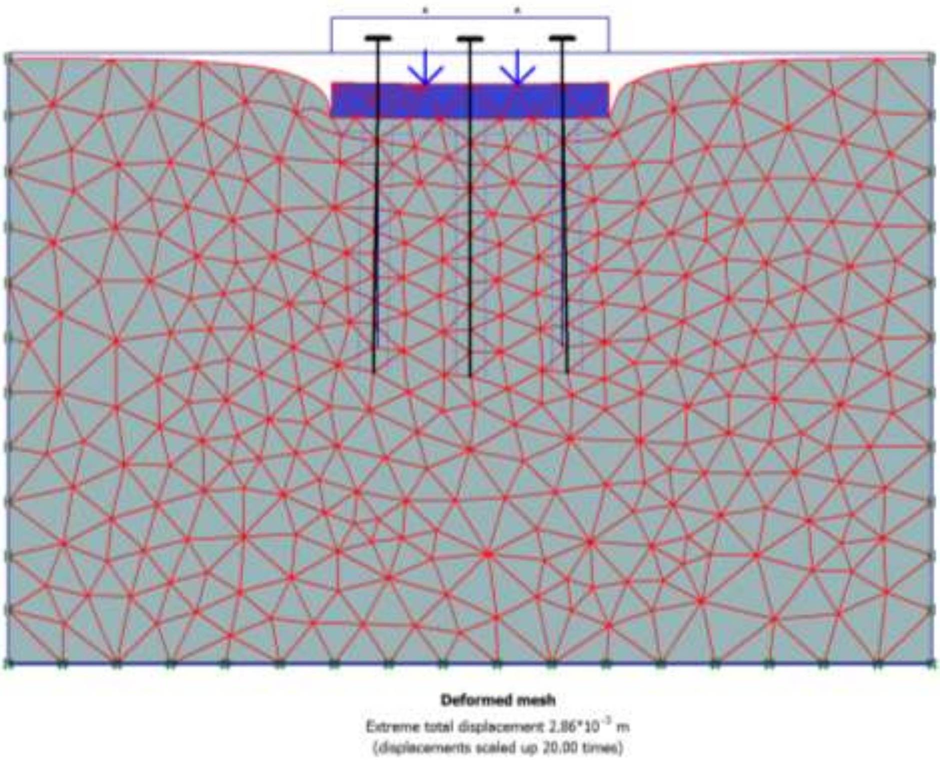

Figure 11 - Modified structure in the third stage

Amount of tensions

The total tension calculated by the software at various stages is presented below.

First stage

The total stress contours are presented in Fig. 12. The stress level in the foundation varies from 400 to 7600 Nm / m2. The negative sign indicates the stress. Maximum compressive stress occurred at the bottom of the foundation. In fact, the stress created at this stage is simply due to the weight of the soil. For this reason, the foundation is more stressful, as more weight is due to the weight of the material applied to it. As shown in the figure, the tensions increase from a minimum to maximum and is proportional to weight gain.

Received:24January 2018/Accepted:30 April 2018/Published:1 June 2018

International Academic Journal of Science and Engineering,
Vol. 5, No. 1, pp. 170-190.

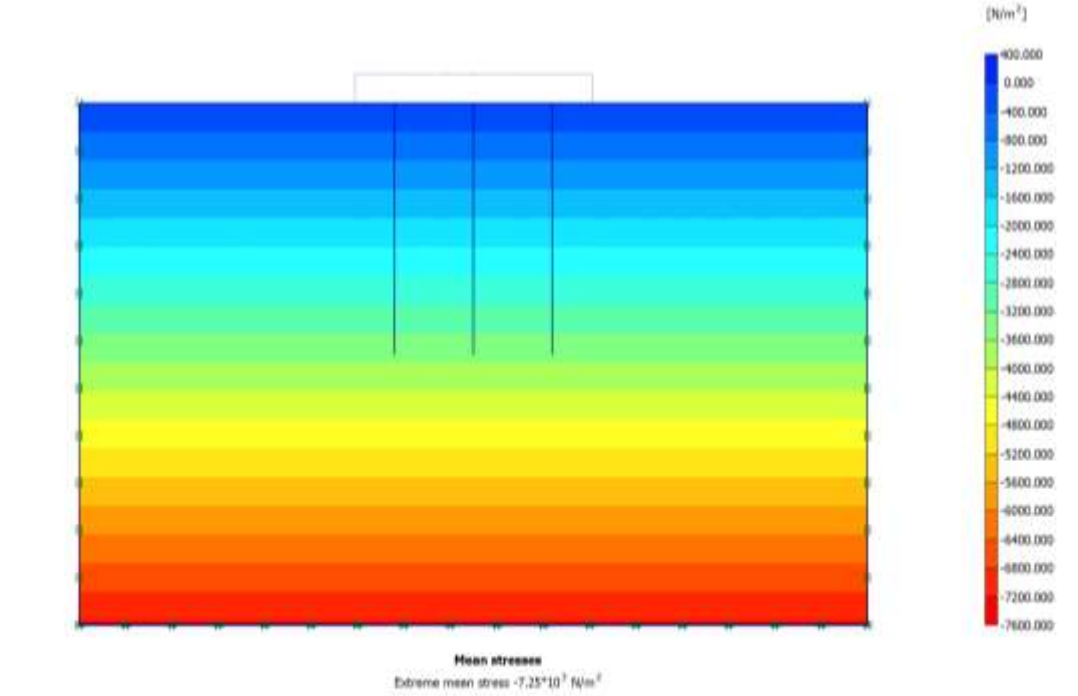

Figure 12 - Total stress contours in the first stage

Second stage

The total stress contours are presented in Fig. 13. The total stress level varies from 160 to 100 kN / m 2. As in the figure, the foundation at this point is at all points in the pressure, due to the effect of the piles and the pressure caused by the presence of the piles. The pile cap is located under bend due to the presence of the piles and partly in the stretching and partly in the pressure. As shown in the figure, the highest pressure has occurred in the bottom of the pile cap, due to the pressure caused by the pile and the warhead. As it is shown in the figure, the stress level underneath the pile cap is reduced from top to bottom, and gradually the tension fades. The tension diagram below the pile cup corresponds somewhat to the form of stress in flexible soils, which shows the correct results of modeling (Fig. 14).

Received:24January 2018/Accepted:30 April 2018/Published:1 June 2018

International Academic Journal of Science and Engineering,
Vol. 5, No. 1, pp. 170-190.

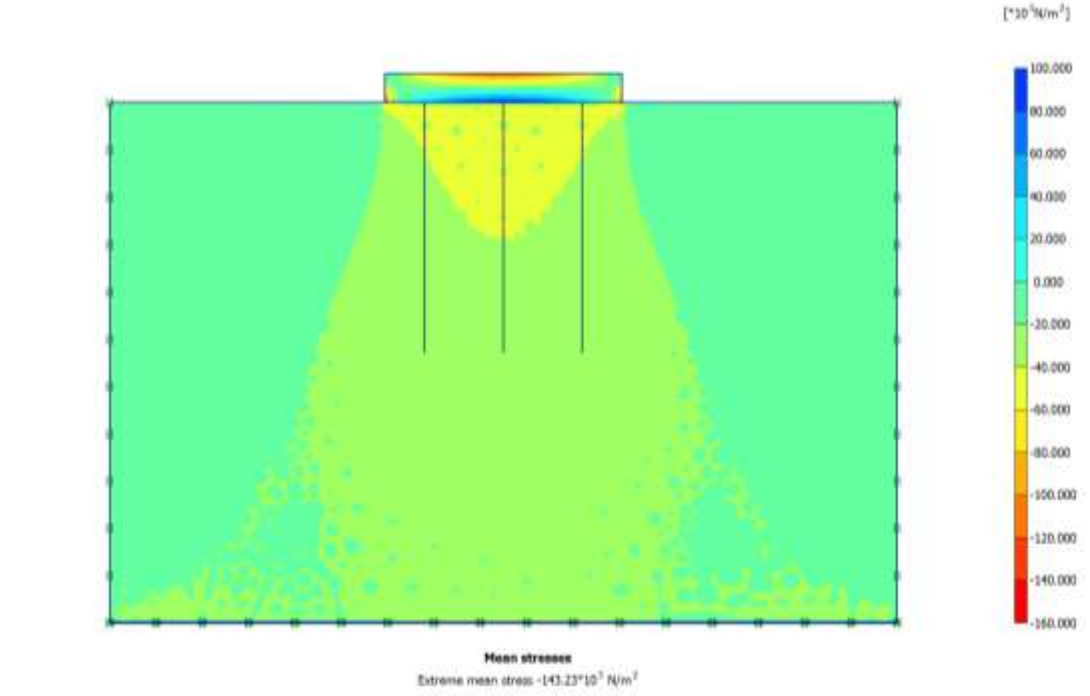

Figure 13 - Total stress contours in the second stage

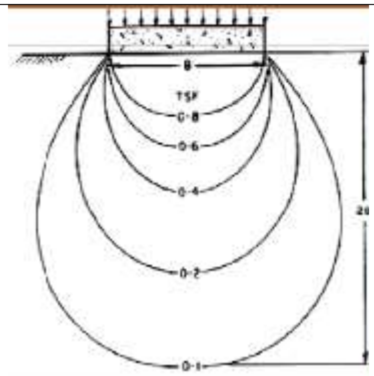

Figure 14 - Distributed stress distribution using analytical methods

Third level

The main stress contours are presented in Fig. 15. The total stress level varies from 1,100 to 500 kN / m 2. As in the figure, there is a uniform stress in the foundation. The pile warhead is similar to the previous stage under bending, and thereafter there are pressures and tensile stresses on the pile holder.

Received:24January 2018/Accepted:30 April 2018/Published:1 June 2018

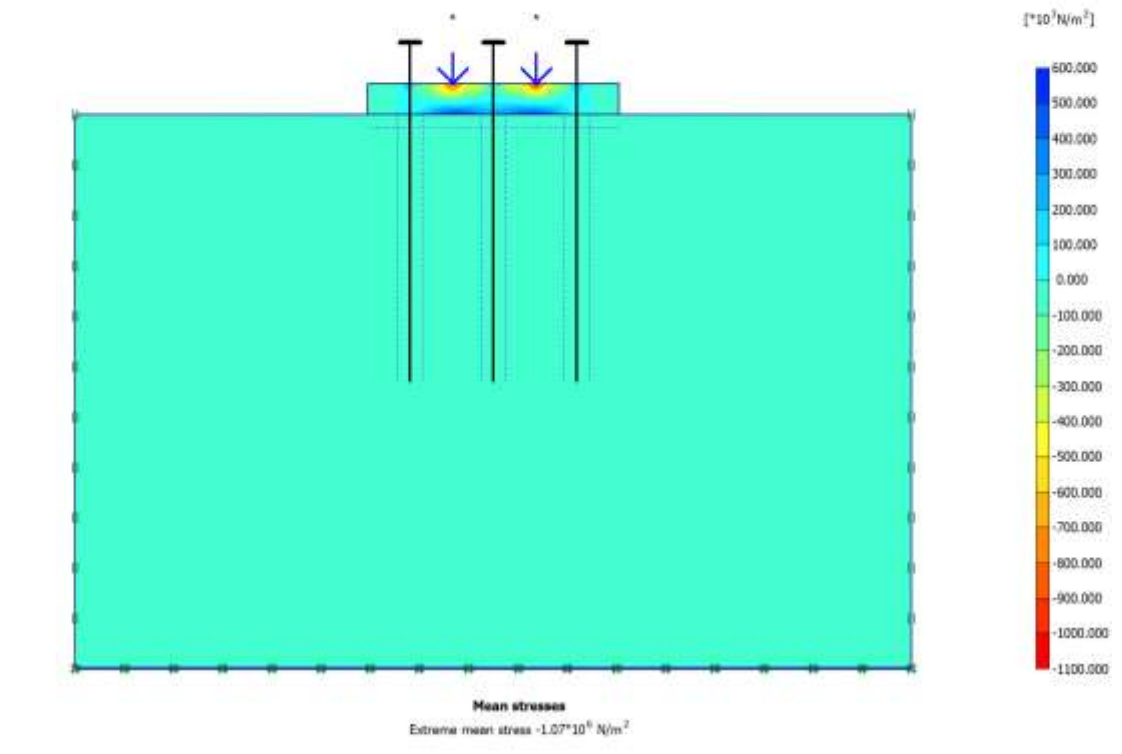

Figure 15 - Total stress contours in the third stage

Verification chart

The verification chart is presented in Figure 16. As shown in the figure, there is a fairly good correlation between the chart of the software and the chart in the article. In the early days, the level of the settlement is very small, with time passing through the tenth day, the settlement will increase with a steep slope. After the tenth day, the settlement has been declining.

Received:24January 2018/Accepted:30 April 2018/Published:1 June 2018

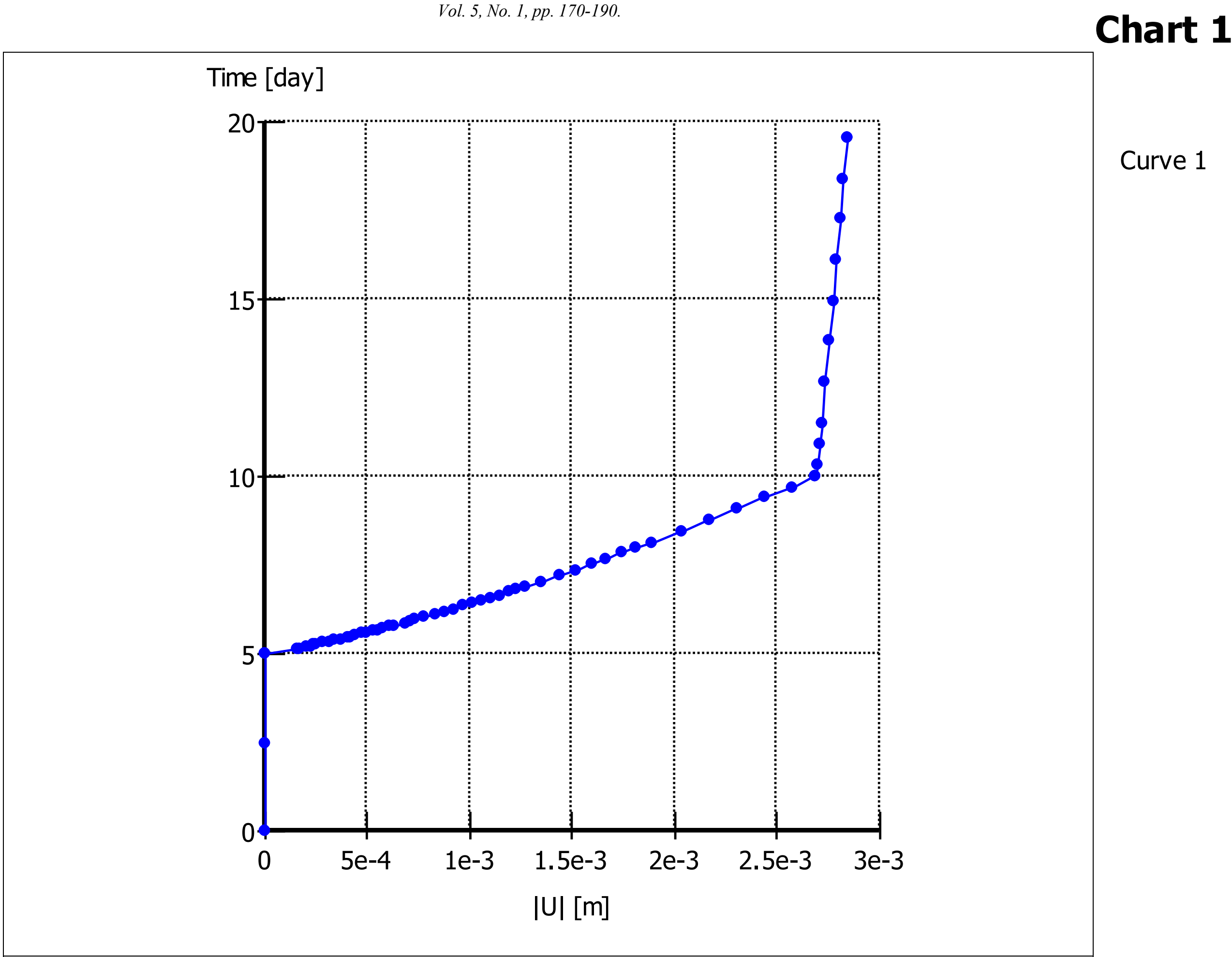

Figure 16 - Verification Schedule

4. Conclusion

The piles are members of steel, concrete, reinforced concrete and wood, which is used to build a deep pile, if the landing capacity is not suitable for use. In spite of high costs, there are many cases in which there are numerous cases of pile sticks used to protect the building against sewage and other factors. The load on the pile is tolerated in two ways by the pile, part of which is tolerated by the side-pile resistance and the other part by the reciprocating tip of the pile. This composite system is called a piled raft system, or a piled raft foundation.

The piles are divided into two groups of displacing piles and replacement piles. Swinging piles are piles that are placed on the ground by knocking or vibration, and replaced by piles in pre-excavated places, prefabricated or in place. A microfiber is a replaceable pile by drilling and injection of cement slurry, which is usually flat and has a micro diameter (usually less than 300mm).

Today, for many reasons, the desire to build heavy and high structures (including residential, commercial, medical, industrial etc.) has increased in most regions. With increasing weight and height of structures,

Received:24January 2018/Accepted:30 April 2018/Published:1 June 2018

other surface foundations (single, strip, wide, etc.) will not be responsive to the forces involved, and in most cases, the use of deep foundations (piles) is required to withstand the loads.

Advantages of using micro-piles in the substrate bed are described in more detail: For new structures, the benefits of micro-polyps can be reduced seating, increased pressure bearing, tensile load and increased lateral load. For existing structures, the control of PIC, load control, repair or replacement of PW, PNP control and seismic retrofit control is noted.

In this study Plaxis finite element software for modeling has been used. The results of the modeling are as follows:

✓ The maximum displacement is about 3 mm, which occurred at the final stage of modeling. In the first stage, the modeling of the level of displacement is very small, due to the graininess of the soil and the dry assumption of the material. In the second stage, the spatial variations show a sudden increase, due to the presence of pile and the weight of the pile holder. In the third stage, the soil is completely compressed, so the force exerted a lot of influence on the summation, and the level of the second and third phase does not differ significantly.

✓ In the first stage, all tensions are compressive and are due to weight of materials and the highest tension is in the foundation. In the second step, the tension below is consistent with those recommended in technical texts, and the tension under the pile's warhead is a bell function. In the third stage, the stress is formed almost uniformly in the foundation, and the pile cap is bent, and partly in the pressure and partly in the stretch. The stress level in the third stage shows a significant increase compared to the stress level in the second stage.

References

Afshar, C., Kalantari, F., Hemmati, Ghorbani, 2008; Assessment of raft bending hardness on the bearing capacity of the piles and the control of the overall and differential separation of raft in the direction of the piled - Raft, 4th- National Civil Engineering Congress, University of Tehran, Iran.

AH Pour, R., Jamei, M., Bina, M., 2010, Case study of the use of injectable micro-pads to control settling in heavy water reservoirs in loose clay soils, Fourth International Conference on Geotechnical Engineering and Soil Mechanics Engineering, Iran , Tehran.

Cadden, A., Gómez, J., Bruce, D., and Armour, T. (2004) Micropiles: Recent Advances and Future Trends. Current Practices and Future Trends in Deep Foundations: pp. 140-165, doi: 10.1061/40743(142)9

Esmaeili-Falak, M., Ramezani Yardi, T. 1391; Investigating the Sewage Effect of Slabs in Susceptible Soils of Psychoanalysis, Regional Conference on Civil Engineering, Malayer.

HAFEZ, D AND ET AL, 2012, SEISMIC RESPONSE OF GROUP OF MICROPILES CONSIDERING PILE-CAP CONNECTIVITY CONDITIONS, Geotechnical Special Publication, ASCE.

Hashemi, H., Divine, H., Saber Mahani, M., 2011, Division of load between pile and soil in Piled Raft foundation system with the use of micro piles, 6th National Congress of Civil Engineering, Semnan University, Semnan, Iran.

Received:24January 2018/Accepted:30 April 2018/Published:1 June 2018

Khushe Charkh, A., Motaqedi, S., Falahat, M., R, 2007, Investigation of the effect of the angle of gravity on the seismic behavior of steel mill, national earthquake conference and building rehabilitation, Behbahan.

Mansouri Kia, M., 2006; Advantages of using microfiber for the construction and stabilization of water structures, National Conference on irrigation and drainage management, Chamran University, Ahvaz.

Moghanloo, R., A., Imani, H., Sahar, H., 2008, Reinforcement, foundation and wall by in situ micro-plugs, First International Conference on Seismic Rehabilitation, Tabriz, Iran.

Nazari M., A., Mahboobi Ardakani, A, R., 2009, Investigating the Seismic Behavior of micro Plates, Eighth International Congress on Civil Engineering, Shiraz.

Noorzad, R., Sahaghi, Gh., R, 2008; Investigation of Seismic Behavior of micro Melting piles, Fourth National Congress of Civil Engineering, University of Tehran.

Omid Ali, H., Mohammadi, S., Fakhr, A., 2011, Influence of piles on static behavior of microfiber group in piles and decks, Journal of Civil and Surveying Engineering, No. 3, p. 279 to 290 .

Penaghi, K., Mahbubi, A., R., 2010, Analysis of the effect of the distance of piles in a pile group on impedance and transfer functions in a model for soil- pile interaction, Fifth National Congress of Civil Engineering, Ferdowsi University of Mashhad, Mashhad.

Qamari, A., Ghorbani, A., 2010, Real scale experiment and numerical modeling of micro -sized pile in sandy soil, 4th International Conference on Geotechnical Engineering and Soil Mechanics, Tehran, Tehran.

R, Ramezani Yardi, F, R, Dynamic Analysis of Seismic Performance of micro Plumbers, First National Conference on Geotechnics, Ardebil.

Rajabi, A., R., Heydari, M., 1392, Investigating the interaction of structure-soil- pile on the response of a pile under earthquake load, National Conference on Computational Techniques and Optimization in Civil Engineering, Saqez.

Rasaei, et al., 2011; 2011; studying the behavior of climbing behavior under vertical load in sandy soils, 6th National Congress of Civil Engineering, Semnan University.

Salehi Malekshahi, S., Islami, A., 1392), Geotechnical performance of composite piled raft system with consideration of the variables of soldered pile, Sharif Civil Engineering Magazine, Volume 2-29, Issue 2.

Sirifian, S., Darabi, M., 2010, Technical and Economic Comparison of Common Cylinders and Micro Piles (Micro Films) in Coastal Structures Using Case Studies, Fourth International Conference on Geotechnical Engineering and Soil Mechanics, Tehran

Taylor, G. E., Gularte, F. B., and Gularte, G. G. (1998). Seismic retrofit of Fourth Street & Riverside viaducts with micropiles, In: A. Maher and D. S. Yang (eds.). Soil Improvement for Big Digs, Geotechnical Special Publication No. 81, ASCE, Reston, Virginia. pp. 313–325.

Zelenko, B. H., Bruce, D. A., Schoenwolf, D. A. and Traylor, R. P. (1998). Micropile applications for seismic retrofit preserves historic structure in old San Juan, Puerto Rico, In: L. Johnsen and D. Berry (eds.). Grouts and Grouting, Geotechnical Special Publication No. 80, ASCE, Reston, Virginia. pp. 43–62.

Received:24January 2018/Accepted:30 April 2018/Published:1 June 2018